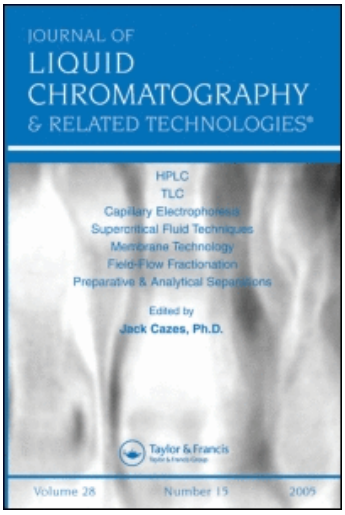

Journal of Liquid Chromatography & Related Technologies
Publication details, including instructions for authors and subscription information:
http://www.informaworld.com/smpp/title~content=t713597273

Separation of Charged Latex Particles by Electrical Field-Flow Fractionation

Martin E. Schimpf[a]; Dale D. Russell[a]; J. Kathleen Lewis[a]
[a] Department of Chemistry, Boise State University, Boise, Idaho

To cite this Article Schimpf, Martin E. , Russell, Dale D. and Lewis, J. Kathleen(1994) 'Separation of Charged Latex Particles by Electrical Field-Flow Fractionation', Journal of Liquid Chromatography & Related Technologies, 17: 14, 3221 — 3238
To link to this Article: DOI: 10.1080/10826079408013200
URL: http://dx.doi.org/10.1080/10826079408013200

JOURNAL OF LIQUID CHROMATOGRAPHY, 17(14&15), 3221-3238 (1994)

SEPARATION OF CHARGED LATEX PARTICLES BY ELECTRICAL FIELD-FLOW FRACTIONATION

MARTIN E. SCHIMPF*, DALE D. RUSSELL, AND J. KATHLEEN LEWIS
Department of Chemistry
Boise State University
Boise, Idaho 83725

ABSTRACT

The retention of both underivatized and carboxylated polystyrene latex beads by electrical field-flow fractionation (ElFFF) was investigated using a 2 mM aqueous solution of quinone-hydroquinone as the carrier liquid. The quninone-hydroquinone redox couple passes current with less polarization of the electrodes than carrier liquids previously employed. Underivatized beads, ranging in diameter from 0.15 to 0.74 μm eluted in the normal mode, while carboxylated beads larger than 1 μm eluted in the steric mode. Normal mode retention increases with flow rate, probably due to shearing of the polarization layer, which increases the working field. At a constant field and flow rate, normal-mode retention is inversely related to the product of a particle's size and electrophoretic mobility, in accordance with retention theory. Thus, ElFFF can be used to obtain both the size and electrophoretic mobility of particle suspensions.

INTRODUCTION AND BACKGROUND

Electrical field-flow fractionation (ElFFF) was introduced in 1972 as a promising method for the separation of proteins (1). However, retention and resolution fell short of theoretical predictions. One problem was polarization of the electrodes by buffers used to dissolve the proteins and carry current across the channel. Polarization caused the channel to behave like a capacitor, with most of the potential drop occurring within a short distance from the channel walls, leaving a very weak field in the bulk of the channel. Polarization was overcome by increasing the field, but the electrodes had to be separated from the channel proper by a porous surface, which allowed current to flow while minimizing the effect of electrolysis products. Unfortunately, the porous surface reduced uniformity in the channel walls and resolution remained poor (2). Later channels were designed with more rigid surfaces (3) to improve channel uniformity, but performance remained significantly below expectations, and the method remained unproductive for over a decade.

In 1990, renewed interest in ElFFF was stimulated by the work of Gau and Caldwell, who developed a new channel design and the methodology for separating charged particles (4). In their design, current-conducting walls serve as electrodes for generating the electrical potential across the channel. Polarization is reduced by adding the redox couple quinone-hydroquinone to the aqueous carrier liquid.

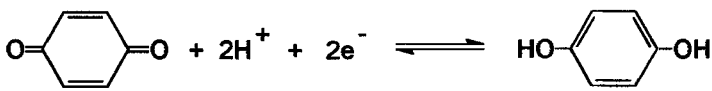

Since no new products are generated in electrode reactions with this redox couple, concentration gradients are not established and polarization of the electrodes is reduced. Using a simple 1.5 volt battery as a power supply, the new system was used to separate underivatized polystyrene particles.

Motivated by their success, Caldwell and Gau built their next-generation channel of resin-impregnated graphite (5), which has the advantage of being both rugged and inexpensive while offering low resistance to current flow. Although the graphite channel failed to yield consistent retention with the quinone-

hydroquinone carrier liquid, other electrolyte solutions were shown to produce efficient separations as long as the ionic strength was kept low. Using the graphite channel, Caldwell and Gau separated a wide range of particles sizes, and demonstrated the expected linear dependence of retention time on field strength.

In the work reported here, we further characterize the retention behavior of underivatized polystyrene latex beads, as well as carboxylated polystyrene, using the quinone-hydroquinone carrier liquid. Our experimental configuration is based on the original design of Gau and Caldwell (4), using gold-coated glass plates as the channel walls. We characterize the dependence of retention on field strength, flow rate, and the size and electrophoretic mobility of the particles.

THEORY

Retention in ElFFF, like other FFF techniques, is based on the application of a force field perpendicular to the separation axis of a thin channel. The field, which is applied across the thin dimension of the channel, interacts with analyte, forcing it to one of the walls (referred to as the accumulation wall). Due to viscous drag, the velocity is reduced toward the walls, and therefore the volume V_r of carrier liquid required to flush the analyte through the channel is related to analyte interactions with the field. Several comprehensive summaries of FFF retention theory can be found in the literature (see for example references 5,6), including those specific to ElFFF (7). Below is a condensed summary of the relevant concepts and equations applicable to ElFFF.

There are two forms of particle retention in FFF; they are referred to as the "normal" and "steric" modes. In both forms, a zone of injected particles is forced to the accumulation wall through interactions with the field. In the normal mode, Brownian motion of the particles cause them to back-diffuse from the accumulation wall toward the center of the channel. A balance is struck whereby the field-induced motion and back-diffusion are balanced, and the zone relaxes into a dynamic but steady-state distribution of particles in which the concentration is highest at the accumulation wall and decreases exponentially toward the center of the channel. The thickness ℓ of the compressed zone is related to the magnitude of the voltage drop ΔV applied across the channel and to the diameter d and electrophoretic mobility μ of the particles

$$\lambda = \frac{l}{w} = \frac{kT}{3\pi\eta} \cdot \frac{1}{\mu d} \cdot \frac{1}{\Delta V} \quad (1)$$

Here kT is the thermal energy, w is the channel thickness (typically 0.1-0.2 mm), and η is the viscosity of the carrier liquid. The ratio l/w is termed the retention parameter λ, and is fundamental to all FFF techniques.

Because flow of the carrier liquid is laminar, λ can be related precisely to the volume V_r of carrier liquid required to flush the zone through the channel

$$R = V^o/V_r = 6\lambda[\coth(1/2\lambda) - 2\lambda] \quad (2)$$

Here V^o is the geometric volume of the channel and R is termed the retention ratio. When retention is sufficiently strong ($R < 0.2$), equation 1 simplifies to

$$R = 6\lambda \quad (3)$$

Equations 1 and 3 can be combined to yield

$$V_r = \frac{\pi\eta V^o}{2kT} \cdot d\,\mu\,\Delta V \quad (4)$$

As indicated by equation 4, smaller particles generally elute ahead of larger ones in the normal mode (i.e. they have a smaller retention volume). This is because their Brownian motion carries them further from the accumulation wall, where the carrier liquid is moving at a higher velocity through the channel. Larger particles, on the other hand, move more slowly through the channel because they are compressed more tightly against the accumulation wall, where the velocity of the carrier liquid is reduced.

Previous studies indicate that much of the applied voltage ΔV is lost by polarization of the electrode walls, so that the working field responsible for particle retention is significantly reduced. For example, when the carrier liquid is a 49 μM aqueous solution of NaCl (conductivity 5 μS/cm), more than 99% of the applied potential is dropped across the polarization layers (5). As the ionic strength of the carrier liquid is increased, polarization becomes more severe, and retention

decreases accordingly. A potential method for combating the buildup is to increase the flow rate of carrier liquid in order to perturb the polarization layers via shearing action of the carrier flow.

When the particle size and/or voltage drop is sufficiently large, the particles are forced to the wall so strongly that the magnitude of l approaches the size of the particles. When this occurs, Brownian motion is negligible and the physical size of the particles governs how far they protrudes into the faster flow lines. In this steric mode of retention, the elution order reverses, with larger particles eluting ahead of smaller ones. The relationship between steric-mode retention and particle size is given by the following approximate expression (8)

$$V_r = \frac{wV^o}{3} \cdot \frac{1}{d} \tag{5}$$

In order to quantify the ability of FFF to separate particles according to their size, we define the size-based selectivity s_d as follows

$$s_d = \left| \frac{d \ln V_r}{d \ln d} \right| \tag{6}$$

In both the normal and steric mode, V_r is related linearly to particle diameter, so that s_d is expected to have a value of unity. The transition between the normal and steric modes is fairly abrupt. In the transition region, selectivity is diminished. At the inversion diameter (9), which is the particle size where the elution order reverses, s_d falls to zero. Particle size distributions that span the inversion diameter are difficult to characterize because two different particle sizes coelute. Fortunately, the inversion diameter can be shifted somewhat by adjusting experimental conditions (10), such as flow rate and field strength. However, for separating samples having extremely broad size distributions, it may not be possible to shift the inversion diameter outside of the distribution, and a pre-fractionation must be performed in order to obtain two or more fractions that can be subsequently separated individually.

MATERIALS AND METHODS

The ElFFF channel is illustrated in Figure 1. A 76 μm-thick mylar spacer is sandwiched between two glass plates that have been coated with gold by vacuum deposition. The glass plates are clamped between two sheets of Plexiglass using several bolts to provide a leak-proof seal. Holes in the plates provide an inlet and outlet to the channel, which is 37 cm long, 2 cm wide and 76 μm thick; the resulting void volume V^o is 0.65 mL. Sample and carrier liquid enter and exit the channel through pieces of Teflon tubing that are friction fit to the holes. An injection valve with a 3 μL loop for sample loading is connected to a four-way manual switching valve and mounted near the channel inlet. The switching valve allows the flow of carrier liquid to be routed around the channel during a stop-flow procedure, in which flow in the channel is halted after sample injection to allow the particles to reach their equilibrium distribution at the accumulation wall in the absence of downstream flow. The stop-flow procedure eliminates band broadening associated with sample relaxation (11), resulting in more efficient separations. By comparing retention times and peak areas using different stop-flow times, we found that 6 minutes of stop-flow time was sufficient for all experiments.

The gold faces of the channel are charged with a 20-volt adjustable power supply whose output is attenuated 20:1 by a voltage divider built in-house. The voltage supply is wired to five contact points along the length of each glass plate to provide a uniform field. The channel is placed in a vertical position so that gravitational forces do not affect retention. The carrier liquid is delivered with a single-piston HPLC pump, and the channel effluent is monitored with a variable wavelength UV detector set at 270 nm. The detector signal is sent to a chart recorder for visual display of the fractogram.

The carrier liquid was a solution of 2 mM quinone in deionized water, adjusted to pH 4.7 with HCl; the resulting solution has a conductivity of 18 mS/cm. The polystyrene latex standards were obtained from Polysciences, Inc. (Warrington, PA). Electrophoretic mobilities were determined on several of the standards (Table 1) using an electrokinetic sonic analyzer (Maytec Instruments, Hopkington, MA), which relies on the generation of a pressure wave by the sample in response to an oscillating electric field.

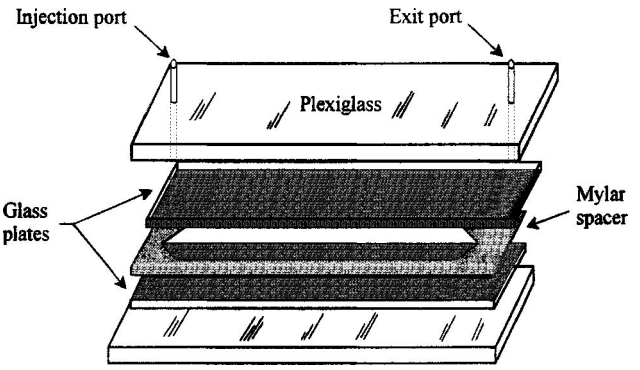

FIGURE 1. Schematic of the ElFFF channel.

TABLE 1.

Electrophoretic Mobility μ of Underivitized and Carboxylated Polystyrene Latex Standards.

	Diameter (μm)	Mobility (10^4 $cm^2s^{-1}V^{-1}$)
Underivitized Polystyrene	0.15	1.77
	0.22	2.26
	0.37	2.35
	0.48	1.83
	0.74	1.40
Carboxylated Polystyrene	0.10	2.05
	0.21	2.53
	0.55	2.29
	0.79	2.12
	1.07	1.32

RESULTS AND DISCUSSION

According to equation 4, retention parameter λ should vary inversely with the magnitude of the working field when the normal mode of retention is at work. Consequently, as the field is increased, λ should decrease toward a limiting value equal to the radius of the particle. Figure 2 plots a series of λ-values, measured at various field strengths, on an underivatized polystyrene (UPS) standard having a diameter of 0.37 μm. Fields above 1 V lead to irregular peaks and an irregular baseline, presumably due to gas bubbles formed by the electrolytic decomposition of water. Between 0.3 V and 1.0 V, the expected linear increase in λ with 1/V is observed. However, the slope is much larger than predicted by equation 1 because the working field is much less than the applied field. Thus, the abscissa in Figure 2, which reflects the applied field, is greatly compressed compared to the range of working 1/V-values. Based on the particle's electrophoretic mobility, equation 1 predicts a slope of 5.6×10^{-4} V for normal-mode retention of the 0.37 μm-diameter standard. The slope in figure 2 is 5.0×10^{-3} V, or 9 times the predicted value, which indicates a working field that is only 11% of the applied field. This compares favorably with the use of NaCl solutions as the carrier liquid, where the working field is only 0.2% of the applied field (5). The precipitous drop in retention (increase in λ) below 0.3 V (3.33 V^{-1} in Figure 2) presumably signifies the charging potential of the two electrode surfaces.

As we discussed above, an increase in flow rate should raise the working field by shearing the polarization layers. We tested this hypothesis on the 0.37 μm UPS standard using a field of 0.3 V. As illustrated in Figure 3, V_r continues to increase with flow rate up to a flow rate of 2.0 mL/min. Further flow increases were not possible due to leakage of the channel. The increase in retention with flow rate is a new factor to ElFFF separations that is not present in other FFF techniques, or in chromatography-like techniques in general. The major outcome of the flow rate dependence of retention is the need to use consistent flow rates in applying calibration curves to the analysis of unknown samples. However, this is a minor inconvenience--consistent flow rates are commonly used anyway. The flow rate dependence must also be considered in methods development. For example, in characterizing an unknown sample by FFF, a preliminary fractogram is often obtained at a high flow rate to determine the proper field strength. The higher flow rate minimizes development time. (One of the advantages of FFF is that the

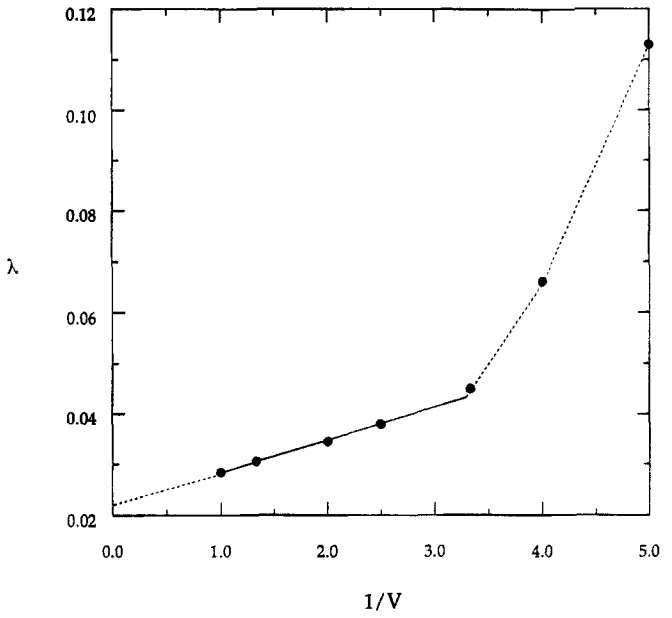

FIGURE 2. Dependence of retention parameter λ on the inverse of the applied voltage V. The sample is a 0.37 μm UPS standard; the flow rate is 1.82 mL/min.

field can be readily controlled and optimized for a given separation.) Once the preliminary run is completed, the required field is easily determined, and the flow is reduced for sample analysis. With ElFFF, either the flow rate used in the preliminary run will need to match that of the analytical run, or the retention dependence will have to be accounted for in determining the proper field strength.

In characterizing sub-micron particles by FFF, a low flow rate is typically used (< 1.0 mL/min) in order to minimize band broadening and thereby maximize resolution. However, the recent trend has been to utilize faster flow rates and/or lower fields in order to decrease run time at the expense of resolving power. Figure 4 illustrates the separation of two polystyrene standards in about 3 minutes using a ΔV of 0.3 V and a flow rate of 1.50 mL/min. Here, the run time was made as short as possible without losing the indication of a bimodal distribution.

According to equation 4, normal mode retention is governed by both size and electrophoretic mobility. For colloidal particles, the electrophoretic mobility in a

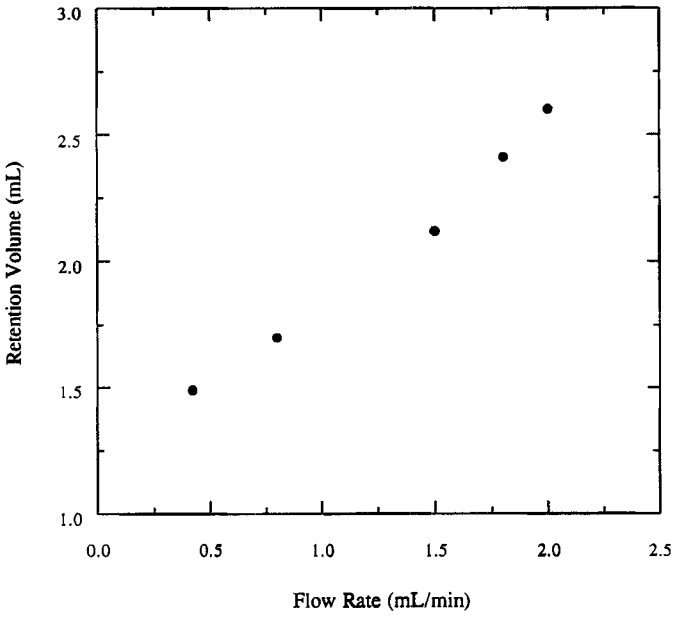

FIGURE 3. Dependence of retention volume on flow rate. The sample is a 0.37 μm UPS standard; the applied potential is 0.30 V.

given medium is fairly insensitive to particle size, provided the surface composition is relatively invariant (12). However, in the submicron size range, a small but measurable size effect on mobility is predicted. Fortunately, the size effect is consistent for a given type of particle, and therefore ElFFF retention can be calibrated to particle size without knowing the electrophoretic mobilities. This is illustrated in Figure 5, where retention volume is plotted against UPS particle size at both low and high flow rates. The curvature in these plots is due to the effect of size on electrophoretic mobility, particularly for the smallest particle (d = 0.15 μm), which has a significantly reduced μ-value. The two plots diverge initially, then parallel one another. The divergence is expected because the magnitude of the working field increases with flow rate and equation 4 predicts an increase in V_r/d with increasing field strength. It is unclear why the plots do not continue to diverge beyond particle diameters of 0.4 μm.

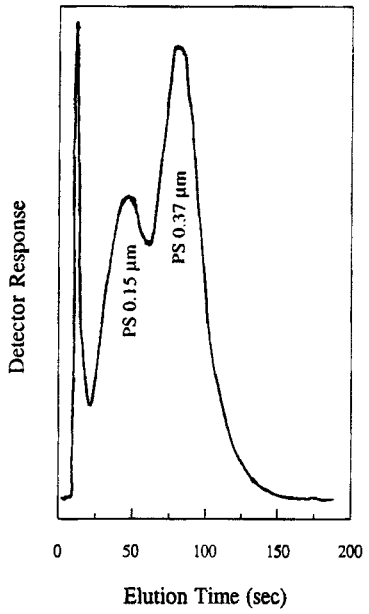

FIGURE 4. ElFFF fractogram illustrating the separation of two UPS standards. The applied potential is 0.30 V; the flow rate is 1.50 mL/min.

Next, we evaluate the retention behavior of several carboxylated polystyrene (CPS) standards ranging in diameter from 0.15 to 4.55 μm. Figure 6 illustrates the dependence of retention on particle size at a flow rate of 1.82 mL/min and a ΔV of 0.3 V. The steric transition occurs at an inversion diameter of 1.0 μm. As discussed in the Theory section, when particles are compressed into layer thicknesses approaching the size of the particle, their retention is determined by physical exclusion from the wall. When this happens, the elution order is reversed, and larger particles elute ahead of smaller ones. Based on the value of λ (0.03) where inversion occurs, the most highly retained particles are still 2 μm from the channel wall, a distance which is significantly greater than their radius of 0.5 μm. The additional exclusion distance is due to two factors -- a large double layer on the particles, as a result of the low ionic strength of the carrier liquid, and lift forces at the accumulation wall. Although lift forces are not well understood, they are known to elevate the particle from the wall, resulting in decreased retention.

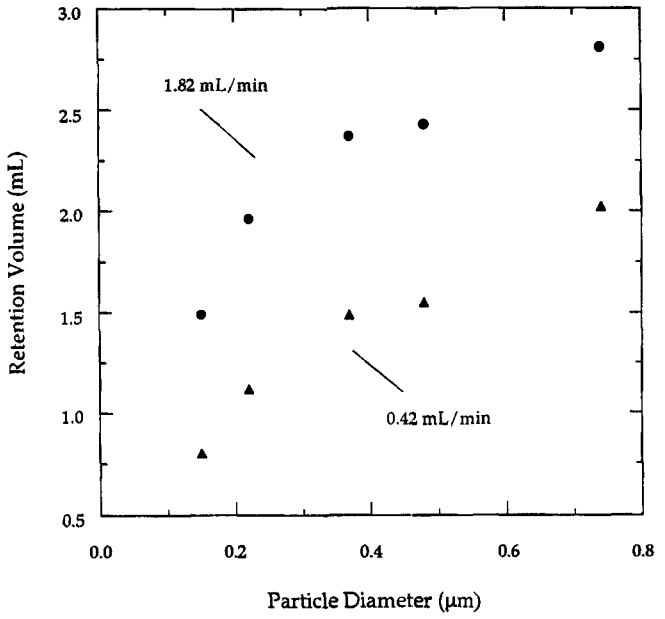

FIGURE 5. Dependence of retention volume on particle size of UPS standards at low and high flow rates. The applied potential is 0.30 V; the flow rate is 1.82 mL/min.

In the normal mode, lift forces are not a factor; in the steric mode, the lift force is a function of many factors, including the particle size and flow rate of the carrier liquid. The increase in lift force with particle size is responsible for the non-linear dependence of retention on particle diameter in the steric mode, as illustrated in Figure 6.

As we mentioned in the Theory section, we expect a size-based selectivity of 1 in both the normal and steric modes, based on the definition given in equation 6. (In the steric mode, lift forces cause the selectivity to drop from a maximum of 1 with increased particle size.) Experimentally, we obtain selectivities that are only about 0.6 in the normal mode for both UPS and CPS. In the steric mode, the data is limited, but the selectivity is approximately 0.6 near the inversion diameter. While the size-based selectivity is affected by a slight dependence of electrophoretic mobility on size, this does not account for the discrepency. The

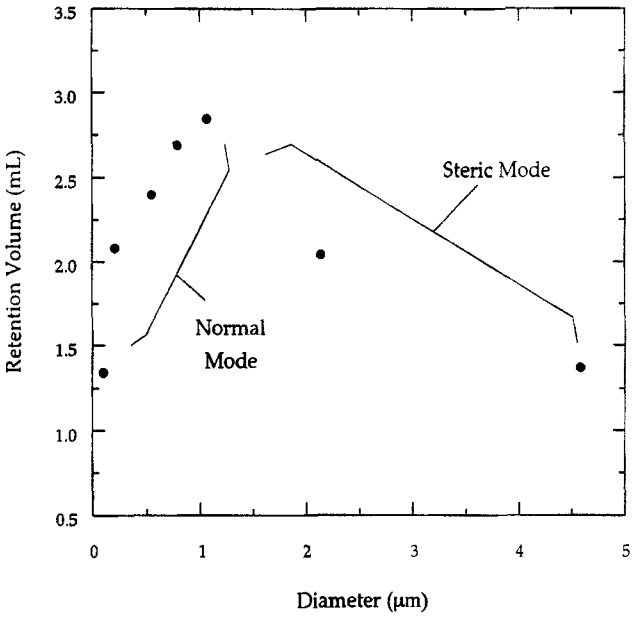

FIGURE 6. Dependence of retention volume on particle size of CPS standards. Both normal- and steric-mode retention are illustrated. The applied field is 0.30 V; the flow rate is 1.82 mL/min.

reason for the reduced selectivity remains unclear. However, one contributing factor is the presence of double layers surrounding the particles, which should add significantly to their effective size in the low ionic strength mediums used in this work. The double layer thickness should be fairly uniform over the size range examined, so the apparent selectivity, which is calculated using core diameters, will be artificially low.

A mixture of particles having a size range that spans the inversion diameter can lead to erroneous information on particle size. As an example, the fractogram illustrated in Figure 7 was obtained on three CPS standards; the particle sizes are 0.10 μm, 0.55 μm, and 2.1 μm. The center peak contains the larger standard, which elutes in the steric mode with a retention volume that is intermediate between the other two standards. Suppose the particle sizes were unknown and this fractogram was used to establish the size distribution based on the calibration

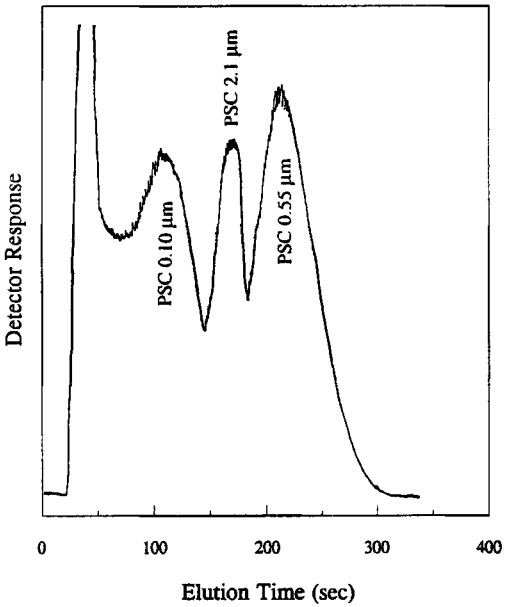

FIGURE 7. ElFFF fractogram illustrating the separation of three CPS standards. The center peak contains a standard that has eluted in the steric mode. The applied field is 0.30 V; the flow rate is 1.02 mL/min.

curve in Figure 6. One might assign the center peak a diameter of 0.2 µm, which coelutes in the normal mode with 2 µm particles eluting in the steric mode. An experienced FFF practitioner might suspect the center peak because it is particularly narrow compared to the other two. Often, however, polydisperse samples elute as a single broad peak, which may or may not contain particles coeluting in both modes of retention. Fortunately, an experienced FFF user can also identify coelution in broad distributions by a steep edge on the high-V_r side of the elution profile. For a detailed discussion on the coelution of particles in the normal and steric modes, the reader is referred to reference 10.

If we compare the normal-mode retention of CPS to that of UPS, we find that CPS retention is slightly greater than that of similarly sized beads of UPS, at the same flow rate and field strength. For example, the retention volume of 0.21 µm CPS particles is 2.08 mL, while that of 0.22 µm UPS particles is only 1.96 mL.

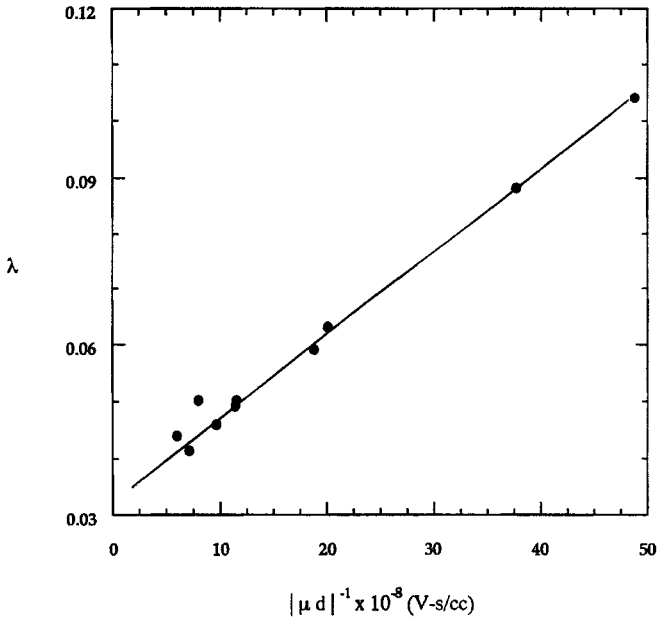

FIGURE 8. Dependence of retention parameter λ on the inverse product of the electrophoretic mobility μ and particle diameter d. The applied potential is 0.3 V; the flow rate is 1.82 mL/min.

The difference lies in their electrophoretic mobilities, which are slightly higher in CPS. The larger electrophoretic mobilities translate into a stronger force driving the CPS particles to the accumulation wall, hence greater retention in the normal mode. If the electrophoretic mobilities are known, retention of different particle types can be represented by a single calibration plot of retention parameter λ versus the reciprocal product of particle diameter and electrophoretic mobility. Such a plot is illustrated in Figure 8. Here, the retention data on CPS is combined with the UPS data taken at the same flow rate of 1.82 mL/min. Since the field strength, flow rate, and carrier-liquid composition were held constant for all the data, a linear relationship is obtained, in accordance with equation 1. The slope of the plot in Figure 8 is 1.4×10^{-11} cc/V-sec; equation 1 predicts a slope of 1.6×10^{-12} cc/V-sec. As was the case in Figure 2, the discrepancy lies in the magnitude of the working field, which is greatly reduced from the applied potential

by polarization of the electrodes. Comparing the slope in Figure 8 with that expected from theory indicates a working field that is 11% of the applied field, consistent with previous indications.

Caldwell and Gau demonstrated that polarization differs with the nature and conductivity of the carrier liquid. As we have shown, the flow rate is also important, and certainly we can expect the nature of the electrode surface to be a factor. However, by careful control of the field strength, as well as the nature and flow rate of the carrier liquid, Figure 8 illustrates the potential of ElFFF for characterizing charged particles. If the particle size is known, ElFFF can be used to obtain electrophoretic mobilities, and even distributions in μ. By measuring retention under several different sets of experimental conditions, both size and electrophoretic mobilities could be obtained by ElFFF. Finally, if ElFFF is used in combination with a light scattering detector, both the size and electrophoretic mobility could be obtained from a single fractogram.

CONCLUSIONS

The newly designed ElFFF channel shows potential as an alternative method for analyzing charged particles. The channel is inexpensive and easy to assemble. The major difficulty with the technique lies in the dependence of retention on parameters that influence polarization of the electrodes. As a result, several parameters associated with the carrier liquid must be carefully controlled in addition to the field strength. With the 2 mM quinone-hydroquinone carrier used in this work, critical parameters include the flow rate, pH, and conductivity. Although 89% of the field is lost at the electrode surface due to polarization of the electrodes, applied potentials of less than one volt still result in efficient separations of both micron and sub-micron sized particles whose electrophoretic mobilities are in the range of 10^{-4} cm^2/V-s.

In the work reported here, we obtained a size-based selectivity of ~0.6, which is significantly lower than the expected value of unity predicted by retention theory. Caldwell and Gau reported a selectivity of ~0.7 using a solution of NaCl as the carrier liquid. However, the apparent discrepancy between theory and experiment probably arises from the double layer on the particle, which is not accounted for in empirical determinations of selectivity. If instead of using core

diameters to calculate selectivity, the thickness of the double layers were known and accounted for, the apparent selectivity would increase. Nevertheless, for measuring core diameters, the selectivity is lower than other FFF techniques, including flow FFF and sedimentation FFF. Yet, flow and sedimentation instruments are significantly more expensive than ElFFF equipment, so the reduced selectivity may well be worth the cost savings for many applications.

The unique feature of ElFFF is its ability to separate particles based on their charge, or electrophoretic mobility. While the resolution of the technique is comparable to that of capillary zone electrophoresis (CZE) (5, 13), the speed of CZE is significantly greater. However, ElFFF can deal with much higher sample loadings than CZE, which is conducive to sample collection and subsequent analysis by secondary methods, such as photon correlation spectroscopy. The two-dimensional capability that becomes available when fractions can be collected may be critical for analyzing unknown samples of a complex or polydisperse nature.

ACKNOWLEDGMENTS

We thank Dr. Karin Caldwell and Dr. Yu-Shu Gau for their valuable counsel. We thank Hewlett-Packard Corp. for supporting the initial work, and for their assistance in determining particle mobilities. This work was supported by the NSF-Idaho EPScOR program and by National Science Foundation grant number OSR-9350539.

REFERENCES

1. K. D. Caldwell, L. F. Kesner, M. N. Myers, J. C. Giddings, Science 176: 296 (1972).

2. L. F. Kesner, K. D. Caldwell, M. N. Myers, J. C. Giddings, Anal. Chem., 48: 1834 (1976).

3. J. C. Giddings, J. C. Lin, M. N. Myers, Sep. Sci., 11: 553 (1976).

4. Y.-S. Gau, K. D. Caldwell, The Second International Symposium on Field-Flow Fractionation, Salt Lake City, Utah, 1991.

5. J. C. Giddings, J. Chem. Phys., 49: 81 (1968).

6. M. N. Myers, J. C. Giddings, Anal. Chem., 54: 2284 (1982).

7. K. D. Caldwell, Y.-S. Gao, Anal. Chem., 65: 1764 (1993).

8. J. C. Giddings, M. N. Myers, Sep. Sci., 13: 637 (1978).

9. J. C. Giddings, M. H. Moon, Anal. Chem., 64: 3029 (1992).

10. S. K. Ratanathanawongs, J. C. Giddings, in Chromatography of Polymers: Characterization by SEC and FFF, T. Provder, Ed., ACS Symp. Series No. 521, American Chemical Society, Washington, DC, 1993, pp. 47-62.

11. M. E. Schimpf, M. N. Myers, J. C. Giddings, J. Appl. Polym. Sci., 31: 117 (1987).

12. D. C. Henry, Proc. R. Soc. Lodon, Ser. A, 133: 106 (1931).

13. S. L. Petersen, N. E. Ballou, Anal. Chem., 64: 1676 (1992).

Received: November 8, 1993
Accepted: January 7, 1994